Experimental comparison of two testing setups for characterizing the shear mechanical properties of masonry

Jorge Segura[a*], Ernest Bernat[b], Virginia Mendizábal[b], Luca Pelà[a], Pere Roca[a], Lluís Gil[b]

[a] Department of Civil and Environmental Engineering, Universitat Politècnica de Catalunya (UPC-BarcelonaTech), 08034 Barcelona, Spain

[b] Department of Strength of Materials and Structures in Engineering, Universitat Politècnica de Catalunya (UPC), 08222 Terrassa, Spain

Abstract: The prediction of the structural capacity of masonry buildings against lateral loads requires an accurate characterization of the masonry strength and general response under shear stresses. The experimental determination of shear strength parameters typically relies on shear tests on wallettes, or on standard triplets. Aiming to avoid the behavioural interpretation problems related with the existence of two mortar joints in triplets, this paper investigates the alternative possibility of testing simple couplet specimens. A direct experimental comparison was established with tests on the two specimen configurations (triplets and couplets) performed on two different types of masonry, both characterised by low strength mortars (hydraulic lime and cement based). The obtained results include the evaluation of Mohr-Coulomb parameters, residual shear strengths, second mode fracture energy, and secant shear modulus. The findings point out that couplets yield consistent experimental results and provide systematically higher estimations of all parameters compared to triplets.

Keywords: shear strength; triplet test; couplet test; masonry; hydraulic lime mortar; clay brick; cohesion; friction; fracture energy; dilatancy.

Highlights:

- Standard triplet tests for shear characterization are compared to simple couplets.
- Couplets provide consistent experimental results and predict similar trends.
- Couplets provide systematically higher estimations of all shear parameters.
- Observations from two different types of masonry are consistent between them.
- Shear parameter estimations for a historical-like brickwork are provided.

1 Introduction

Earthquakes, wind, support settlements or unsymmetrical distributions of vertical loads constitute actions that subject buildings to in-plane shear loading [1]. Under these conditions, the evaluation of the masonry shear strength is of great importance to accurately assess the structural performance of the building [2].

The shear strength of a masonry wall depends on a number of factors [3], such as the wall aspect ratio, the mechanical properties of the components - i.e. units and mortar-, the bond tensile strength of the joints, the boundary conditions, and the compression stress level experienced by the wall. Zhang and Beyer [4] and Malomo et al. [5] have also investigated the role played by the bond pattern. Nevertheless, it is accepted that a key parameter in the shear resistance of a wall is the shear strength of the bed joints. The vast amount of research carried out along the last decades [6] has established as a consensus that the joint shear failure at low precompression levels can be adequately described by the Mohr-Coulomb (MC) criterion, expressed herein by Equation 1:

$$\tau_u = c + \sigma \tan \phi \quad (1)$$

where the ultimate joint shear strength τ_u and the normal compressive stress σ are related by means of the cohesion c and the internal friction angle ϕ. In the common case of failure through the unit-mortar

interface, the cohesion can be interpreted as the initial bond at zero precompression τ_0, while the tangent of the angle of friction represents the coefficient of friction μ.

Different testing configurations have been proposed for the experimental determination of the Mohr-Coulomb parameters [7–9]. Riddington et al. [10] identified a series of quality criteria that an ideal testing setup should fulfil: *i*) ensure a uniform distribution of normal and shear stresses; *ii*) when failure is initiated at one point, the majority of the joint should be close to failure; *iii*) tensile stresses should be avoided along the joint; *iv*) the failure should be initiated away from the edge of the joint, and *v*) the testing setup should be kept as simple as possible. Yet, as stated by Popal and Lissel [11], none of the currently available methods meets the five criteria. In particular, the first criterion on uniformity -that is the basic assumption for the computation of the acting stresses along the joint- has been found nearly impossible to satisfy [12,13].

With the previous considerations in mind, tests on triplet specimens conformed by three units and two bed joints stand as a compromise solution and have been adopted by most of the national and international standards. The European standard EN 1052-3 [14] gives guidance on the preparation of the specimens, the testing machine, the test method and the calculation method. One of the proposed procedures involves testing groups of specimens at different precompression levels and finding the cohesion and the angle of friction by a linear regression.

The triplet test has been largely applied in both the research and the industrial fields and is used to characterize many different materials (e.g. masonry made of solid [15] and hollow bricks [16], stone units [17] or concrete blocks [16]). Nevertheless, even if generally accepted, this method presents certain inconsistencies derived mainly from the fact that the tested specimen includes more than one joint. Indeed, the assumed symmetry of both specimen and setup may be only apparent since several sources of asymmetry arise: imperfections in the geometry of the units and particularly in the thickness of the mortar joints; irregular boundary conditions, especially with regard to the applied

precompression; the scattering of the properties of the materials including the variation in the roughness of the units' faces and the possible heterogeneity within the mortar.

In consequence, as reported by a number of authors [18–20], both joints do not fail simultaneously. This circumstance is found experimentally [21–23] in force-displacement curves that present two peaks, each of them representing the failure of one of the two different joints. This 'two-peak-phenomenon', as identified by Vermeltfoort [13], hinders the interpretation of the results and raises doubts on which area should be considered for the calculation of shear stresses [24]. In addition, Angelillo et al. [25] have highlighted the impossibility to obtain accurate postpeak characteristics, and Riddington and Jukes [26] have pointed out some practical concerns associated to the size, weight and fragility of the triplet specimens.

An alternative to overcome the limitations of tests on triplets can be found in testing specimens with a single bed joint, hereafter called 'couplets' [27–31]. Many researchers have proposed specific and complex testing setups on couplets [31,32], with the aim of fulfilling the first four of the aforementioned Riddington criteria. Van der Pluijm [33] designed a testing configuration with special metal devices. This latter setup allowed improving the knowledge on the shear behaviour of bed joints and has been successfully and continuously utilised for the calibration of numerical models [20]. However, it has been hardly used in laboratory afterwards given the specificity of the test arrangement, together with some difficulties [6] related to the need of attaching the steel sections to the bricks and the occurrence of a diagonal crack through the centre of the specimen instead of a joint failure for certain types of units.

The main purpose of the research presented herein is to explore the possibility of testing couplets with the simplest setup, i.e. a simple modification of the standard triplet arrangement, and to correlate results obtained with both types of specimen. Although some authors have compiled inventories of shear tests that reported examples from either triplets or couplets [6,34,35], very few

references have dealt with their direct experimental comparison. Lawrence [30] and Schubert and Caballero [36] obtained higher values of cohesion in couplets tests. Conversely, Fouchal et al. [37] found very similar results for both types of specimen. More recently, Zhang et al. [20] presented a numerical evaluation.

This paper presents a preliminary study that describes an experimental programme on triplets and couplets and compares the obtained results in terms of Mohr-Coulomb parameters, i.e. cohesion and angle of friction, but also with regard to fracture energy, deformability and force-displacement curves. Two different material combinations have been considered, both with low strength mortars. The choice of the components of one of the combinations has been intended to represent a historical-like type of masonry. Therefore, the results obtained may contribute, as a secondary objective, to expand the database on shear properties available for this type of material.

2 Experimental programme

2.1 Materials

The experimental programme was carried out at the Materials and Structures Laboratory of Innovation Technology of the Technical University of Catalonia in Terrassa, Barcelona (UPC – BarcelonaTech).

As mentioned, the tests involved two different material combinations to carry out the comparison between triplets and couplets. The first combination was chosen to represent a historical-like type of masonry. Given the difficulties to evaluate the shear properties of existing masonry structures [15], this campaign provided an opportunity to contribute with results obtained through standard triplet tests. Handmade fired solid bricks were selected, with average dimensions 311 (length) × 149 (width) × 45 (height) mm^3. These bricks presented rough surfaces because of their manual way

of manufacturing. A NHL 3.5 natural hydraulic lime based commercial mortar was chosen. The mortar was modified with limestone filler additions to reduce its strength, as explained by the authors in a recent publication [38]. The volume ratio of commercial premixed mortar to filler to water was 1:1:0.65. This material combination of bricks and mortar has been already studied in compression, with results similar to historical ones [39]. On the other hand, the second type of masonry was designed to have different properties but keeping the low strength of the mortar. Modern materials were used in this case, which included a M7.5 Portland cement based commercial mortar and conventionally extruded solid clay bricks, with smooth surfaces and average dimensions 270 × 127 × 51 mm^3. The volume ratio of commercial premixed mortar to water was 1:0.25 [40].

The two sets of materials were conveniently characterized according to EN 772-1 [41], EN 772-6 [42], EN 772-21 [43] and EN 1015-11 [44]. Table 1 summarizes the components' strengths. Full bricks were tested in bending. From the halves, squared specimens of dimensions 100 x 100 mm^2 were cut and tested in compression. Mortar prisms of dimensions 160 x 40 x 40 mm^3 were casted during the construction of the masonry specimens and were tested in bending and in compression at the same age of the masonry specimens. As planned, strengths were different for the two material combinations, with lower strengths in the case of historical-like materials. Nevertheless, the strength of the cement-based mortar can still be considered as a low strength. The variability found in the strength values, with a coefficient of variation up to 28 % in the case of the flexural strength of extruded bricks, is common in these types of materials [45].

Table 1 Mechanical strengths of masonry components. Number of specimens and coefficients of variation are shown in brackets

Material	*Compressive strength (MPa)*	*Flexural strength (MPa)*
Handmade brick	17.99 (20, 8.3%)	2.44 (10, 20.0%)
Extruded brick	27.93 (30, 19.0%)	5.99 (15, 28.0%)
Hydraulic lime mortar	1.02 (12, 22.1%)	0.33 (6, 25.3%)
Portland cement mortar	2.53 (12, 5.7%)	1.03 (6, 9.9%)

2.2 Specimens preparation

Two types of specimen were built for each material combination: standard triplets consisting of three bonded bricks with two mortar joints, and couplets consisting of two bonded bricks with one mortar joint. Figure 1 displays the dimensions of each specimen type.

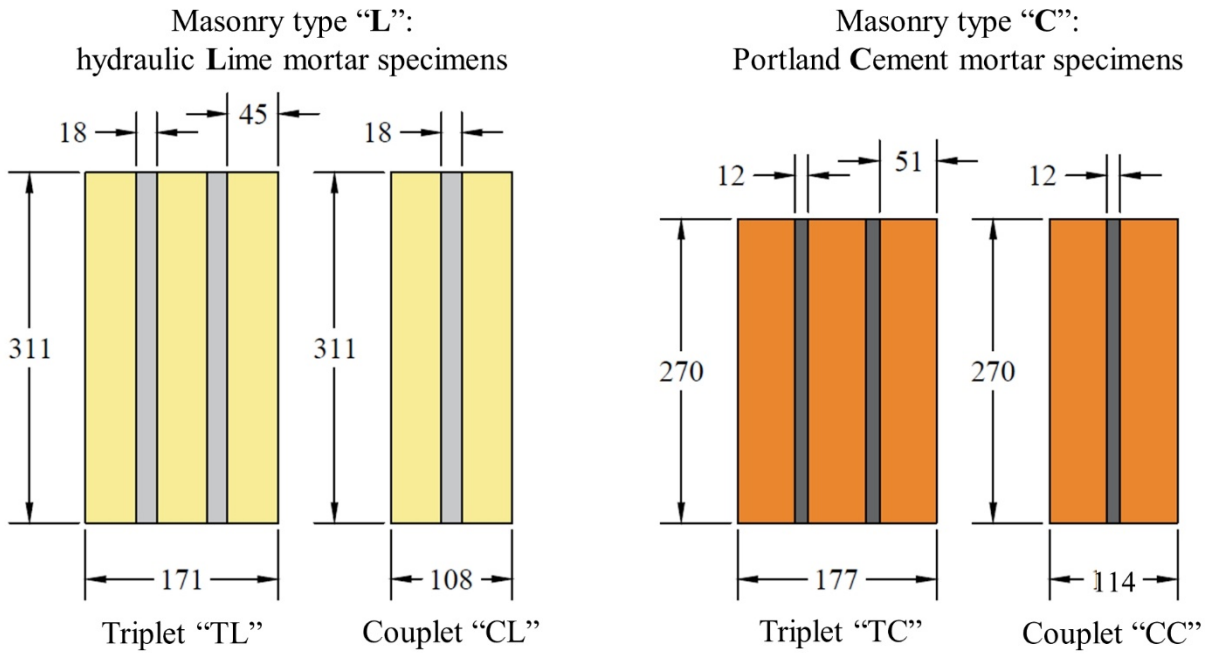

Figure 1 Geometric definition of the masonry specimens

The construction of the specimens included brushing the bricks, especially the handmade ones, wetting them by immersion into water for at least 1 minute (to reduce absorption ratio below

0.0016g/(min·mm²) according with ACI-530 [46]), levelling the first brick, which was laid horizontally on its main side, and placing the next brick(s) on top maintaining the specified mortar joint thickness by using wooden mechanical gages. Average joint thicknesses of 18 mm and 12 mm were selected for the hydraulic lime and the cement mortar respectively. The former was necessary to accommodate the irregularities of the handmade brick surfaces [45], whereas the latter is more representative of real Portland cement joints in modern masonry. All samples were covered with plastic and cured in the same environmental conditions for 28 days, with average temperature of 23 ºC and average humidity of 62%.

2.3 Setup and testing procedure

Figure 2 sketches the testing setups for both triplets and couplets. The shear load (*S*) was applied through an aluminium profile 40 mm wide at the top of the corresponding brick. This profile was necessary to reduce concentration of stresses and avoid the premature local damage of the bricks. Steel profiles supported the other brick(s). The supporting edges were placed in all cases at 2 mm from the brick-joint interface. This measure aimed at reducing the bending effect in the plane of the joints. The precompression normal load (*N*) was applied through a distribution steel plate 20 mm thick. Contact plates were placed at the external faces of the specimen, against the distribution steel plate and the reaction wall. These plates consisted of soft board sheets rubbed with Vaseline. Their aim was double: avoiding local normal stress concentrations and reducing the friction against the shear load. The latter is of the utmost importance in the case of couplets.

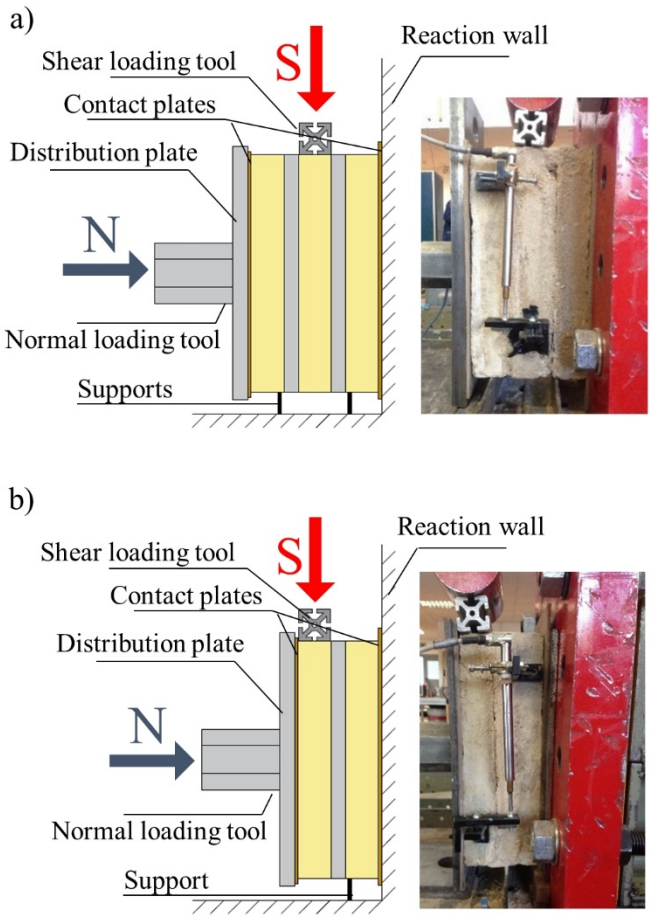

Figure 2 Testing arrangements for a) triplets and b) couplets

Once the specimen was placed in its position, two LVDT sensors with 20 mm range and 0.2% linearity were installed according to Figure 3 to measure the shear vertical (see Figure 2) and normal horizontal deformations. Both sensor support elements and reference contrasting elements were bonded to the brick with cyanoacrylate after convenient polishing and cleaning of the surface.

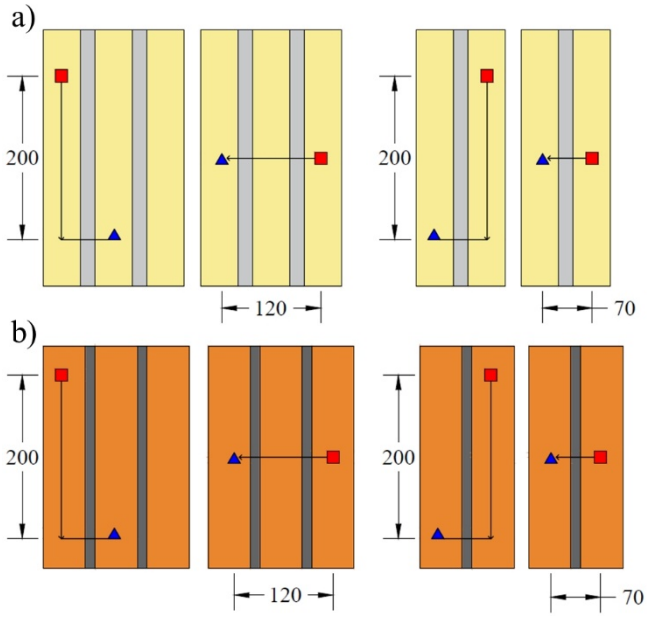

Figure 3 LVDTs position for each specimen type. Red squared dots indicate support of the LVDT, blue triangular dots indicate support of the contrasting element. See Figure 2 for an actual picture of the vertical LVDTs

The tests consisted of two stages. They started with the application of the precompression normal load at a ratio of 10 kN/min. Tests at different levels of normal stress were performed, as indicated in Table 2. The horizontal actuator that applied the precompression load had a maximum capacity of 50 kN. When the precompression load was reached, it was maintained constant during the test, whereas the shear load was indirectly applied as an imposed displacement at a ratio of 1 mm/min. The vertical actuator that applied the shear load had a maximum capacity of 100 kN.

The tests finished when the sensor recording the shear deformation reached its maximum elongation (around 15 mm) and the contact with the reference element was lost. In few cases, this sensor fell from its position due to the energy release associated with the joint failure. In these cases, no full information is available and the corresponding curves are not included in the subsequent analyses.

Table 2 lists all the tested specimens, whose name is a four-position alphanumeric code. The name starts with a letter indicating the type of specimen (“T” for triplets and “C” for couplets),

followed by a letter representing the type of masonry ("L" for masonry made of hydraulic lime mortar and handmade bricks and "C" for masonry made of Portland cement mortar and extruded bricks). The combination of these four letters (TL, TC, CL, CC) in the two first positions of the alphanumeric code defines the four different sets of samples being tested: triplets of hydraulic lime mortar and handmade bricks (TL), couplets of hydraulic lime mortar and handmade bricks (CL), triplets of Portland cement mortar and extruded bricks (TC) and couplets of Portland cement mortar and extruded bricks (CC). The name of the specimens includes also a number that indicates the applied precompression in MPa, and a last number that designates the repetition of the test.

The standard EN1052-3 [14] prescribes to perform tests at three different precompression levels with at least three specimens at each level. This approach has been followed in the case of masonry L. However, taking advantage of the supposed greater homogeneity of the industrialized materials used in TC and CC specimens, it was decided to investigate the convenience of including an additional normal-tangential stresses pair while reducing the repeatability of tests from three to two repetitions. This approach allowed to obtain additional information for the linear regression while saving one specimen. The new level of load considered for specimens TC and CC aimed to represent a zero normal precompression condition. The actual applied stress was 0.01 MPa, and corresponded to the minimum capacity of the horizontal actuator (0.5 kN). This minimum load was necessary to maintain the overturning stability of the specimens during the tests. The values of precompression stress for each test are indicated in Table 2.

Table 2 List of tested specimens and applied normal stresses

Specimen	***Precompression normal stress (MPa)***	***# Repetition***	***Specimen***	***Precompression normal stress (MPa)***	***# Repetition***
TL0.29_1	0.29	1	*TC0.01_1*	0.01	1
TL0.29_2	0.29	2	*TC0.01_2*	0.01	2
TL0.29_3	0.29	3	*TC0.23_1*	0.23	1

TL0.58_1	0.58	1	*TC0.23_2*	0.23	2
TL0.58_2	0.58	2	*TC0.58_1*	0.58	1
TL0.58_3	0.58	3	*TC0.58_2*	0.58	2
TL0.97_1	0.97	1	*TC1.02_1*	1.02	1
TL0.97_2	0.97	2	*TC1.02_2*	1.02	2
TL0.97_3	0.97	3	*CC0.01_1*	0.01	1
CL0.29_1	0.29	1	*CC0.01_2*	0.01	2
CL0.29_2	0.29	2	*CC0.23_1*	0.23	1
CL0.29_3	0.29	3	*CC0.23_2*	0.23	2
CL0.58_1	0.58	1	*CC0.58_1*	0.58	1
CL0.58_2	0.58	2	*CC0.58_2*	0.58	2
CL0.58_3	0.58	3	*CC1.02_1*	1.02	1
CL0.97_1	0.97	1	*CC1.02_2*	1.02	2
CL0.97_2	0.97	2			
CL0.97_3	0.97	3			

2.4 Results

First, it is highlighted that all the specimens failed in the brick-mortar interface by shear sliding, as shown in Figure 4. This failure is one of the valid failures stablished by EN 1052-3 [14], considering two possibilities: either failure on one single interface or on the two interfaces of the mortar joint with a crack across the mortar that connects both sliding surfaces. No clear trend was identified between the type of failure and the component materials, the type of specimen and the precompression stress level.

Figure 4 All specimens failed in the brick-mortar interface either on one or divided between two brick faces, which are types of failure corresponding to failure A.1 described in EN 1052-3 [14]. Examples of different types of specimen:

a) TL, b) CL, c) TC, d) CC. No relationship was observed between type of failure and materials, type of specimen or precompression stress

According to the assumption of uniformity in the stresses distribution made in the EN 1052-3 [14], the shear strength (τ_u) of each specimen was calculated by means of Equations 2 and 3 for triplets and couplets respectively. The normal acting stresses (σ) were calculated for both types of specimen with Equation 4:

$$\tau_u \text{ (Triplets)} = S_{max} / 2A \quad (2)$$

$$\tau_u \text{ (Couplets)} = S_{max} / A \quad (3)$$

$$\sigma = N / A \quad (4)$$

where S_{max} is the maximum shear force attained during the test, N is the precompressive force, and A is the cross sectional area of the specimen parallel to the bed joints. Again, the assumption of uniformity in the stresses is a strong simplification. It is adopted as suggested by the EN 1052-3 [14] and as a commonly accepted disadvantage[12,13].

The pairs of values of shear strength and compressive stress for all the tests are plotted in Figure 5, for the four different sets of samples (TL, CL, TC, CC). Figure 5 also indicates the values of cohesion and angle of friction corresponding to the Mohr-Coulomb failure criterion defined by Equation 1. These parameters have been calculated as the intercept with the τ-axis and the arctangent of the slope, respectively, of a linear regression on the pairs of values.

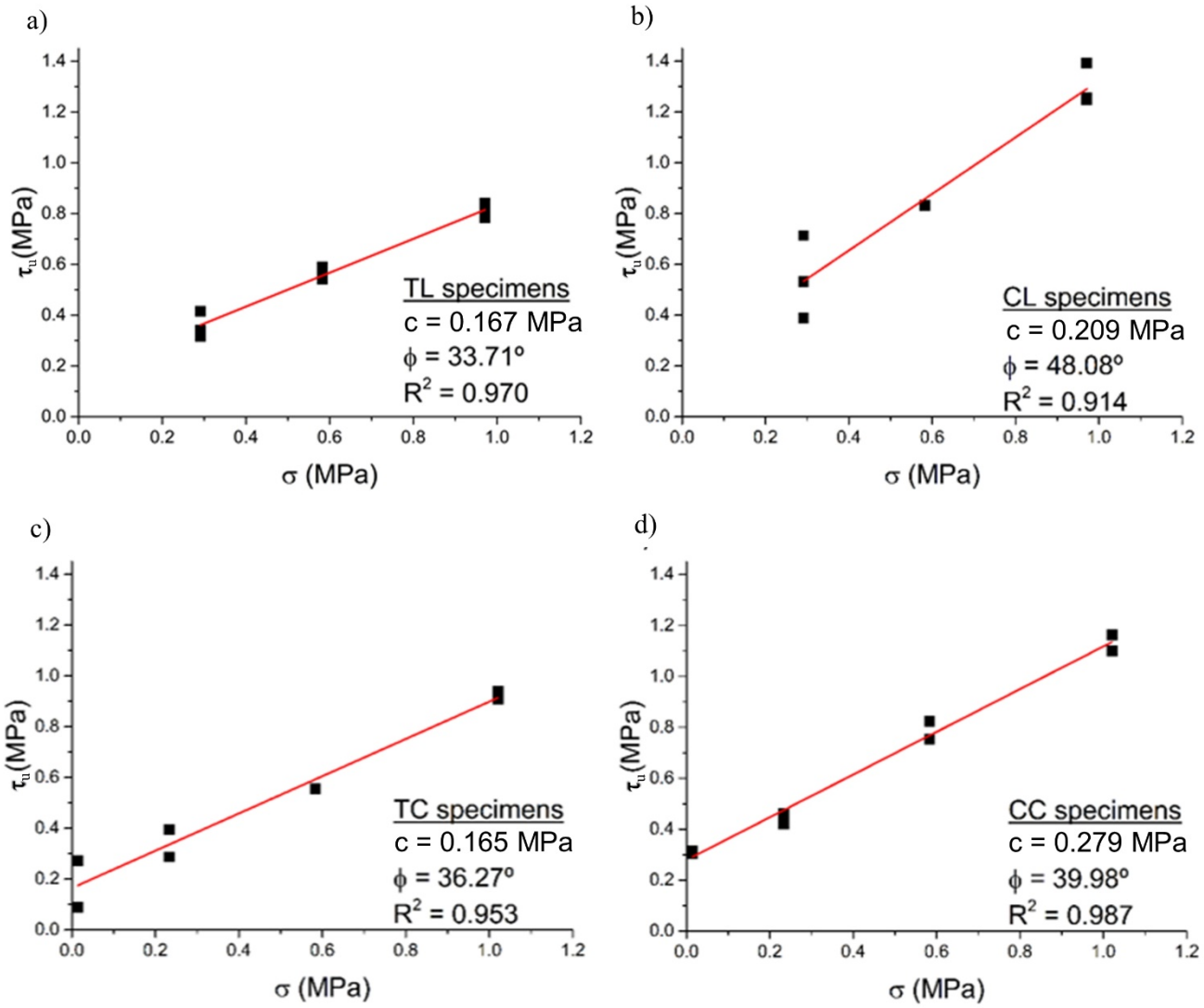

Figure 5 Shear strength τ_u vs. normal stress σ plots for a) TL, b) CL, c) TC, and d) CC specimens. Red lines represent the regression corresponding to the Mohr-Coulomb failure criterion, with indication of the cohesion c, the angle of friction ϕ and the coefficient of determination R^2

Figure 6 and Figure 7 display two types of plot for both masonry combinations. The shear stress recordings along each of the tests are plotted against the relative shear displacement. These curves represent the mechanical response of the joints in shear. The shear displacements are also compared to the displacements measured in the direction perpendicular to the joint. This type of plot captures the possible signs of dilatancy. Dilatancy is the increase of material's volume after crack formation that is associated with the shearing of the joint. In both figures, curves with inconsistent data associated to

measurement issues during the tests are disregarded. Up to 11 curves could not be plotted. Consequently, mechanical parameters depending on deformation were not computed in those cases.

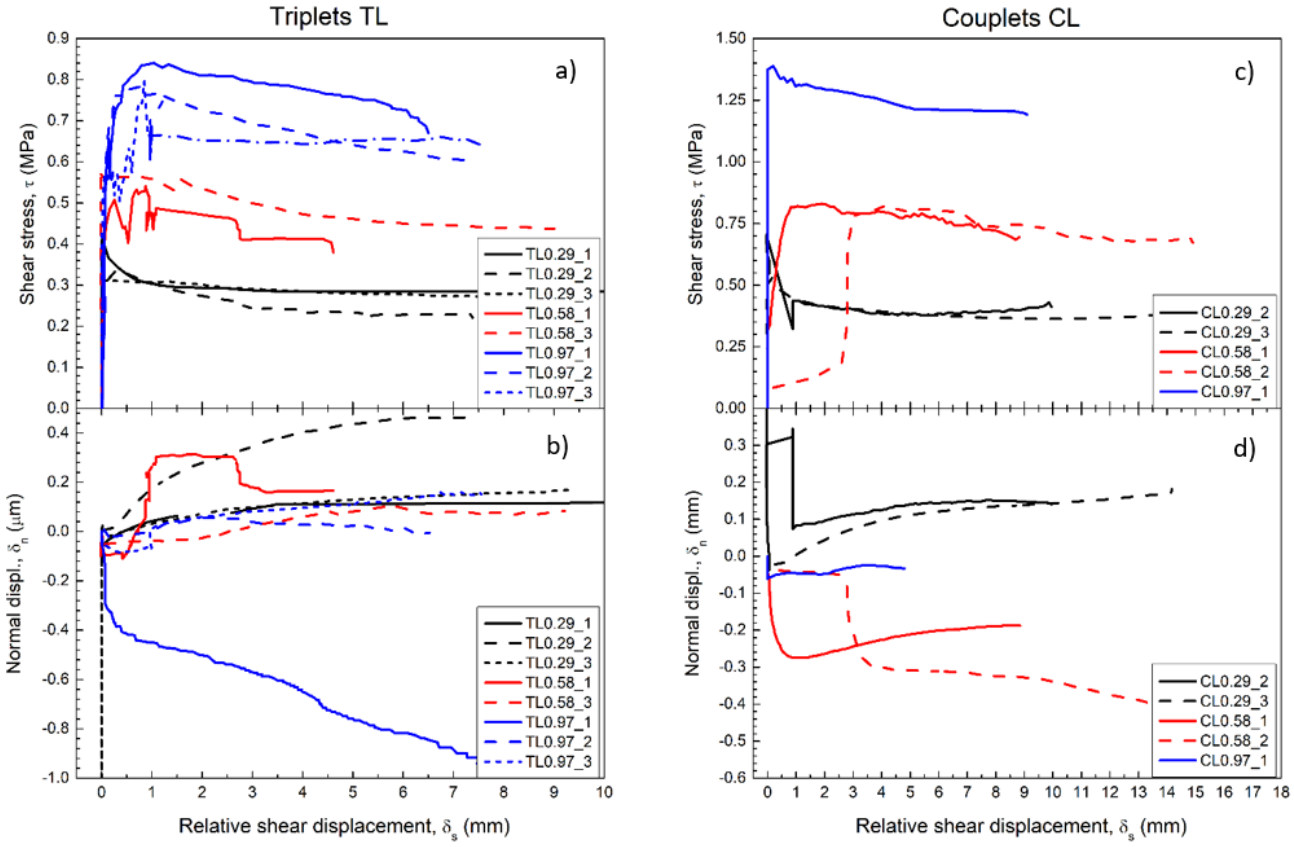

Figure 6 Curves for masonry made of hydraulic lime mortar and handmade bricks. a) Shear stress vs. shear displacement plot for triplets. b) Normal displacement vs. shear displacement plot for triplets. c) Shear stress vs. shear displacement plot for couplets. d) Normal displacement vs. shear displacement plot for couplets

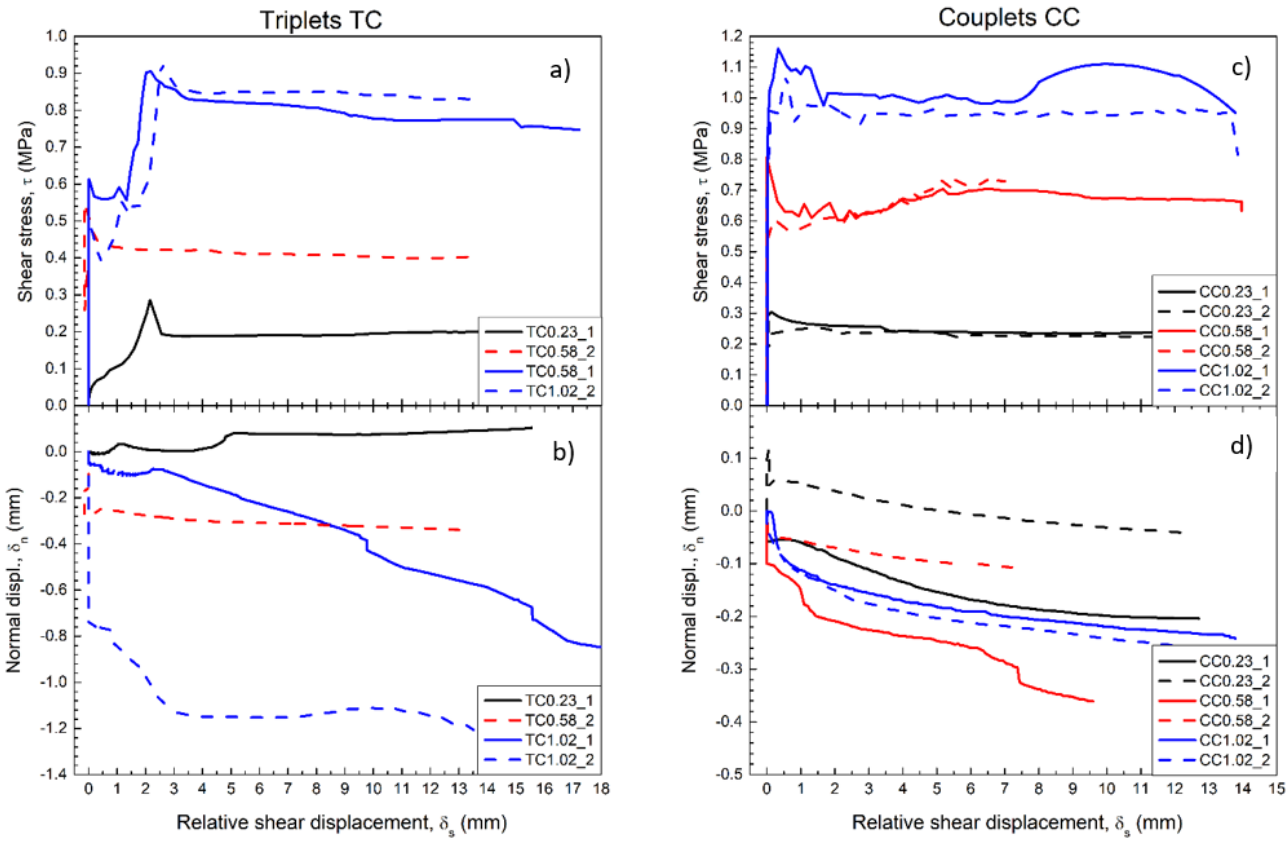

Figure 7 Curves for masonry made of Portland cement mortar and e bricks. a) Shear stress vs. shear displacement plot for triplets. b) Normal displacement vs. shear displacement plot for triplets. c) Shear stress vs. shear displacement plot for couplets. d) Normal displacement vs. shear displacement plot for couplets

Once the peak or ultimate shear strength τ_u was reached and after the failure of the joint(s), the specimens submitted to precompression were able to resist against additional shear deformation. In this research, the residual shear strength τ_{res} has been computed as the measured shear stress for a shear strain of 2.5%. This value of strain allowed the computation of the parameter τ_{res} for most of the tests. The definition of shear strain is given at the end of this section. The residual strength can be compared to the ultimate strength by means of a strength degradation ratio (SDR) as defined by Augenti and Parisi [35] and the following Equation 5. A higher value of SDR corresponds to a lower degradation. Table 3 presents the available results of ultimate and residual shear strength and indicates the

corresponding strength degradation ratio. The two later parameters are used here mainly for comparative purposes between the types of specimen, but residual values play an important role in the evaluation of structures after seismic events.

$$SDR = \tau_{res} / \tau_u \quad (5)$$

Additionally, Table 3 includes the estimated values of the second mode fracture energy. This mechanical property is relevant for the structural analysis of masonry by means of micromodelling approaches [47,48]. Two different procedures have been applied for their calculation, which are schematized in Figure 8. The first procedure follows the common definition as proposed by Van der Pluijm [33] and Lourenço [49] (G_f^{II}, column 6). The fracture energy is estimated as the area below the apex of the shear stress – displacement curves and above the plateau of the residual shear strength. This definition only applies when the shape of the experimental curve is similar to the idealized one of Figure 8a. To overcome the impossibility of computing the fracture energy in some cases, a second approach is proposed. The second procedure defines the fracture energy as the area below the shear stress – displacement curves up to a displacement corresponding to a 2.5% of shear strain ($G_f^{II}{}_{\_2.5\%}$, columns 7 and 8). The first procedure aims to distinguish frictional energy from cohesive fracture energy [50] and evaluates this latter component, whereas the second proposed method involves all energy associated to the failure process for comparable damage final states. For the sake of clarity, these two parameters are called cohesive fracture energy (G_f^{II}) and cohesive-frictional fracture energy ($G_f^{II}{}_{\_2.5\%}$) in the following. The combination of both approaches allows having more objective elements for the comparison between types of specimen.

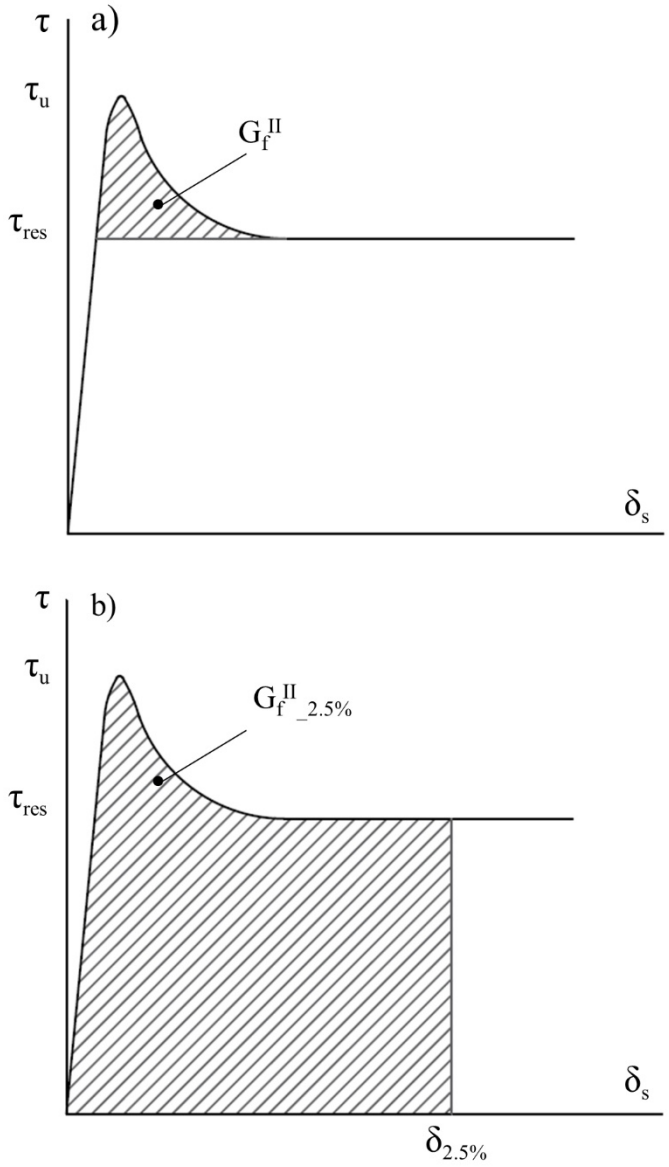

Figure 8 Schematic shear stress τ vs. displacement δ_s curves that show the corresponding areas for the two approaches to calculate second mode fracture energy: a) Cohesive fracture energy G_f^{II}, b) Cohesive-frictional fracture energy taking into account the frictional dissipation up to a displacement corresponding to a 2.5% shear strain $G_{f\_2.5\%}^{II}$

Table 3 Ultimate shear strength τ_u, residual shear strength τ_{res}, strength degradation ratio *SDR*, cohesive fracture energy G_f^{II} and cohesive-frictional fracture energy $G_f^{II}{}_{\_2.5\%}$ for all specimens and precompression levels. The average values for each precompression level of SDR and $G_f^{II}{}_{\_2.5\%}$ are indicated in square brackets

					Second mode fracture energy		
Specimen	τ_u ***(MPa)***	τ_{res} ***(MPa)***	***SDR***		G_f^{II} ***(N/mm)***	G_f^{II}***_2.5% (N/mm)***	
TL0.29_1	0.414	0.285	0.686		0.070	1.566	
TL0.29_2	0.341	0.233	0.685	[0.752]	-	1.364	[1.475]
TL0.29_3	0.316	0.280	0.886		-	1.496	
TL0.58_1	0.541	0.363	0.671		-	2.308	
TL0.58_2	0.557	-	-	[0.737]	-	-	[2.506]
TL0.58_3	0.590	0.473	0.802		-	2.704	
TL0.97_1	0.783	0.629	0.803		-	3.842	
TL0.97_2	0.841	0.756	0.899	[0.853]	0.198	4.003	[3.755]
TL0.97_3	0.810	0.694	0.856		-	3.420	
CL0.29_1	0.388	-	-		-	-	
CL0.29_2	0.713	0.377	0.529	[0.625]	-	2.231	[2.174]
CL0.29_3	0.531	0.383	0.721		0.191	2.117	
CL0.58_1	0.832	0.775	0.931	[0.952]	-	3.861	[2.988]
CL0.58_2	0.830	0.808	0.973		-	2.115	
CL0.97_1	1.393	1.214	0.872	[0.872]	0.380	6.573	[6.573]
CL0.97_2	1.247	-	-		-	-	
TC0.23_1	0.287	0.190	0.661	[0.446]	0.033	0.824	[0.758]
TC0.23_2	0.394	0.091	0.231		-	0.692	
TC0.58_1	0.234	-	-	[0.747]	-	-	[2.220]
TC0.58_2	0.555	0.415	0.747		0.073	2.220	
TC1.02_1	0.908	0.822	0.906	[0.905]	0.076	3.802	[3.660]
TC1.02_2	0.939	0.850	0.905		-	3.517	
CC0.23_1	0.461	0.234	0.508	[0.515]	0.129	1.303	[1.254]
CC0.23_2	0.421	0.220	0.521		-	1.204	
CC0.58_1	0.824	0.673	0.817	[0.817]	-	3.311	[3.217]
CC0.58_2	0.752	0.719	0.956		-	3.122	
CC1.02_1	1.163	1.015	0.873	[0.873]	0.213	5.327	[5.222]
CC1.02_2	1.099	0.942	0.856		-	5.116	

Finally, the secant shear modulus *G* at any point can be calculated by means of Equation 6:

$$G_i = \tau_i / \gamma_i \quad (6)$$

where γ is the shear strain computed as the ratio between the shear displacement and the reference length of the measuring instrument. This definition of shear strain is the one introduced by Augenti and Parisi [35].

Figure 9 displays the evolution of the secant shear modulus for the four sets of specimens.

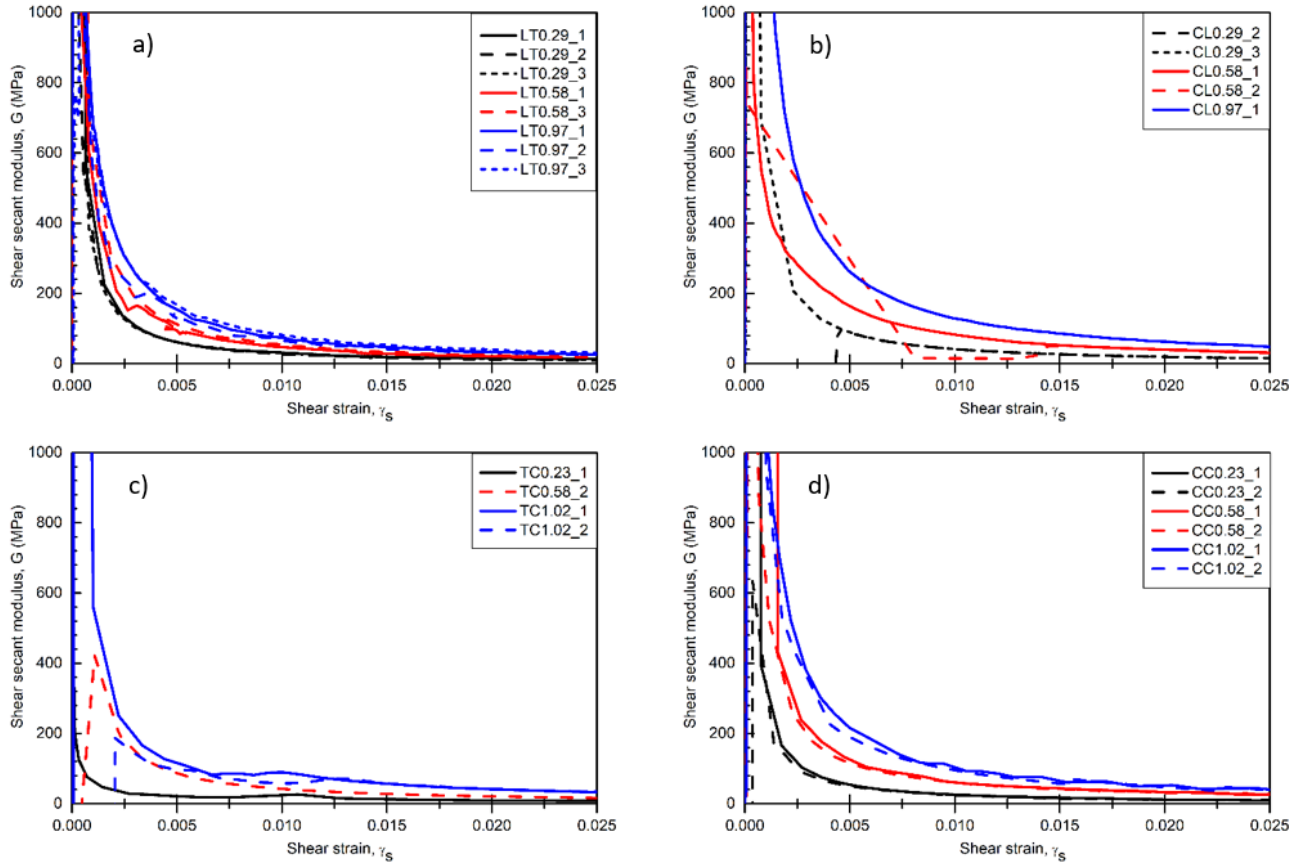

Figure 9 Shear secant modulus G vs. shear strain γ plots for a) TL, b) CL, c) TC, and d) CC specimens

3 Discussion

The discussion of the experimental outcomes is organized in four sections. First, the results are studied from a general point of view. The second section analyses the influence of the type of specimen and compares the results of triplets and couplets. The lasts two sections evaluate the influence of the different materials on the former comparison and present a database of shear mechanical properties for masonry made of low strength mortars.

3.1 General aspects

The results of the four sets of samples show dependency on the level of confining normal stress. This dependency applies for all the parameters, not only for the shear strength and residual shear

strength values, but also for the strength degradation ratio, the fracture energies and the secant shear modulus. Table 3 shows the clear upward trends for each variable. This dependency on the level of confining normal stress was expected due to the frictional behaviour of the material, and has been described by many authors [6,25,35,51].

Figure 5 depicts all the pairs σ-τ_u and the corresponding Mohr-Coulomb envelopes. In three cases (TL, TC and CC) the coefficients of determination R^2 of the regression lines were higher than 0.95. In the single case of couplets made of hydraulic lime mortar and handmade bricks (CL) this coefficient was lower, but still acceptable, with a value higher than 0.9. This can be explained by the inherent variability of the material components, which was evidenced in Table 1 by high coefficients of variation in their mechanical properties. Among the individual data, the results of shear strengths for lower levels of normal stress seem to be more scattered. This is consistent with previous works [15] and is explained because at higher confining stresses the specimens are more stable. In this sense, the high scatter encountered in the samples tested at zero precompression, together with the fact that those tests do not allow the evaluation of postpeak parameters, make advisable to follow the prescriptions of the standard EN1052-3 [14] with regard to the levels of precompression and number of repetitions.

With respect to the stress-displacement curves, Figure 6 and Figure 7 show in general a very stiff behaviour before reaching the peak shear stress. Shear deformation before failure is so small that it is hardly detectable by the installed instruments. In consequence, the curves present quasi-rigid initial branches, as also found by other researchers, e.g. Mojsilovic et al. [52] and Fouchal et al. [37]. This high stiffness is reflected by the vertical asymptotes depicted in the curves of Figure 9, and causes a great difficulty in the measurement of the strain at peak stress. After the peak stress, shear secant modulus is exponentially reduced for all tested cases (see Figure 9). Roca and Araiza [32] also reported similar difficulties to measure the strain at peak stress, finding a significant scattering and even

randomness. Although not able to capture the initial deformation, the installed instrumentation was able to measure the sliding along the joint and thus the postpeak regions of the curves can be considered as reliable. In spite of the difficulties encountered, the general validity of the results for carrying out the comparison between types of specimen is confirmed.

3.2 Influence of the type of specimens

The type of specimens showed to have influence on the determination of all the analysed mechanical properties. The first difference between triplets and couplets is evident when comparing the stress-displacement curves of Figure 6a and Figure 7a, with Figure 6b and Figure 7b. This difference is related to the presence of the additional joint in the triplet specimens. Couplets show a much stiffer behaviour that lasts until the peak stress is reached, while triplets are more deformable and present sometimes the two-peak phenomenon already mentioned in the Introduction section. The non-simultaneous failure of the two joints is manifest, for instance, in the curve of specimen TL0.58_1.

The second and more significant difference is that couplets attained higher shear strengths than triplets for a given level of confining normal stress. Consequently, the estimation of the Mohr-Coulomb parameters was affected. On one hand, the estimated cohesion increased as the shear strength values were higher. On the other hand, the effect of the type of specimen also increased with the confining normal stress, i.e. the greater the confining normal stress, the greater the difference between couplets and triplets. Therefore, the slope of the regression lines changes and so the estimated angle of friction.

These observations partially agree with the few available experimental studies that have previously studied this comparison. Lawrence [30] undertook an experimental campaign on triplet and couplet tests to show up the differences between the two methods. This author found that the shear strength of couplets was higher than the comparative triplet tests. Schubert and Caballero [36] found that the cohesion values estimated in couplet specimens were twice as large the values estimated in

triplets. More recently, Fouchal et al. [37] presented an experimental campaign that involved again these two types of specimen. Although they concluded that both test methods provided similar results, a detailed analysis of their individual data show that couplet specimens gave higher values of cohesion than triplets. However, the three former references dealt with tests performed with zero precompression and their conclusions are not fully comparable to the ones presented herein. The work by Zhang et al. [20] considers different levels of confining normal stresses, but their research is only based on numerical simulations. Under idealized boundary conditions, they found that couplets provided lower values of cohesion but slightly higher values of angle of friction than triplets.

Independently of the previous literature considerations, the differences between triplets and couplets reported in the present research can be justified. Firstly, for the case of zero or low confining normal stresses, Lawrence [30] performed finite element linear analyses to confirm his experimental findings. He investigated the influence of the bending moment created by the non-aligned shear forces in both types of specimen. By comparing the stress distributions along the mortar joints, he found that triplet specimens had a larger region subjected to tension than couplets. Under the hypothesis that bond failure is triggered in the tension regions, this would explain why the shear strength in triplets was lower. Similar stress distributions were determined by Ali and Page [53]. This first argument is only given in terms of qualitative comparison. The findings of Lawrence [30] and Ali and Page [53] were obtained for setups different than the ones used herein. Secondly, as stated by Lei [54], it is an established consensus that brittle fracture obeys the weakest-link postulate. This researcher has validated the existence of a specimen size effect for a wide spectrum of quasi-brittle materials and fracture modes, i.e. an inverse relationship between size and strength attributed to the stochastic distribution of microdefects in a material. Given that the brick-mortar interface area in the two-joint specimens is twice larger than in one-joint specimens, the lower strengths obtained with triplets could also be explained from a statistical approach. Lastly, as for the evaluation of the actual stresses along

the joints, it is worth highlighting again that triplets usually present a double peak phenomenon. It is possible that, at the higher peak, one of the two joints is contributing with the residual strength while the other one has not failed yet. This could lead to an underestimation of the acting shear stress. Conversely, in the couplet specimens, if the friction along the external surface is not negligible, the measured strength could be an overestimation of the actual one. It is likely that both effects occur, which eventually motivates the difference between the two types of specimen.

3.3 Influence of the materials on the comparison between types of specimen

With regard to the two sets of materials being investigated, the tests on standard triplet specimens provided very similar values of cohesion (0.167 MPa for TL specimens and 0.165 MPa for TC specimens) and angle of friction (33.71º for TL specimens and 36.27º for TC specimens). The influence of the different physical properties of each material component is difficult to analyse, as the research on the topic is controversial [6,13]. It could be expected that masonry C, made of cement mortar and extruded bricks, would show a better shear performance given the stronger mortar and the thinner mortar joints. However, the rougher surfaces of the handmade bricks and the higher fineness of the lime mortar aggregates used in masonry L compensate those effects.

In both material sets, the change of testing setup from triplets to couplets resulted in higher values of cohesion and angle of friction although the rates of increase were different. For hydraulic lime mortar specimens, cohesion turned from 0.167 MPa to 0.209 MPa (+25.1%) and the angle of friction varied from 33.71º to 48.08º (+42.6%). In the case of cement mortar specimens, the variations were from 0.165 MPa to 0.279 MPa (+69.1%), and from 36.27º to 39.98º (+10.2%). Even if both variables showed significant increase in both cases, the angle of friction increases more in L specimens, because of the better frictional response due to the roughness of the bricks, while cohesion increases more in C specimens, as they are characterized by better mortar adhesion and smooth surfaces of the

bricks. Finally, it has to be remarked that the absence of an evident trend makes it difficult to find a direct correlation between the results of both types of specimen. This asymmetry in the influence of the type of specimen with respect to the materials has also been observed in the results of Fouchal et al. [37], as the increase in the cohesion values was much higher for hollow bricks than for solid bricks.

A further difference found between materials is the dilative nature of the hydraulic lime mortar specimens. The normal vs. shear displacement plots displayed in Figure 6b and Figure 6d agree with the common features of dilative materials reported by Shadlou et al. [55]: (1) - dilatancy is prevented at small strains and accelerates after yielding at higher strains, as shown by most of the curves that start with a negative slope but change in correspondence with the peak stresses; and (2) – dilatancy depends on the level of normal precompression, as the curves of specimens subjected to the highest normal stresses do not show dilatancy. In the case of cement mortar, all the curves plotted in Figure 7b and Figure 7d present a negative slope and therefore no dilatancy effects were captured. This difference between both materials is related again to the roughness of the bricks surfaces. The handmade ones present an irregular surface as result of the fabrication process. One of their faces is especially rough due to the casting on a layer of sand, so dilatancy is really expected. Conversely, the industrially made bricks present a smooth surface as result of the extrusion process that explains why no dilatancy effects were observed. Moreover, with regard to the comparison between types of specimen, it is significant that both triplets and couplets have yielded the same observations with respect to dilatancy. As expected, the measured absolute magnitude of the normal displacements is higher in the case of triplets than couplets, given than the LVDTs registered the displacements corresponding to two mortar joints instead of one single mortar joint.

Figure 10 provides comparative plots to ease the data interpretation about residual shear strength, strength degradation ratios, and fracture energies. As aforementioned, all the studied parameters show linear dependency on the level of precompression stress. The estimations from

couplet tests are also greater in all cases, except for the strength degradation ratios SDR. With respect to this latter parameter, Figure 10b shows that there is an influence of the material for lower and medium precompression stresses. Indeed, masonry L, which relies more on the contribution of friction, presents higher values of SDR. Eventually, the scattering of the results for higher precompression stresses is significantly reduced and all specimens show similar final SDR, with an average value of 0.87 and a coefficient of variation of 4.2%.

As shown in Figure 10c, a very limited collection of cohesive fracture energy (G_f^{II}) values could be calculated following the previously described first approach. Nevertheless, an estimation of the cohesive fracture energy at zero normal stress can still be done by linear regression. The results for the sets TL, CL, TC and CC are 0.0152 N/mm, 0.110 N/mm, 0.0284 N/mm and 0.104 N/mm respectively. These values are similar or of the same magnitude than those provided in the seminal research of Van der Pluijm [33], with 0.026 N/mm for soft mud brick and 0.058 N/mm for wire cut brick. It is important to note that other than the latter reference mentioned, very few comparative values of second mode fracture energy are available in literature for brick masonry, e.g. Ferretti et al. [21] found a value of 0.011 N/mm for calcium silicate bricks and cement mortar. Regarding the cohesive-frictional fracture energy ($G_f^{II}{}_{\_2.5\%}$) computed with the second procedure, it is noted that specimens built with handmade bricks and hydraulic lime mortar showed greater fracture energy than those made of Portland cement and extruded bricks. This is again likely related with the superficial roughness of handmade bricks that increase the necessary energy to propagate the crack along an irregular superficial contact.

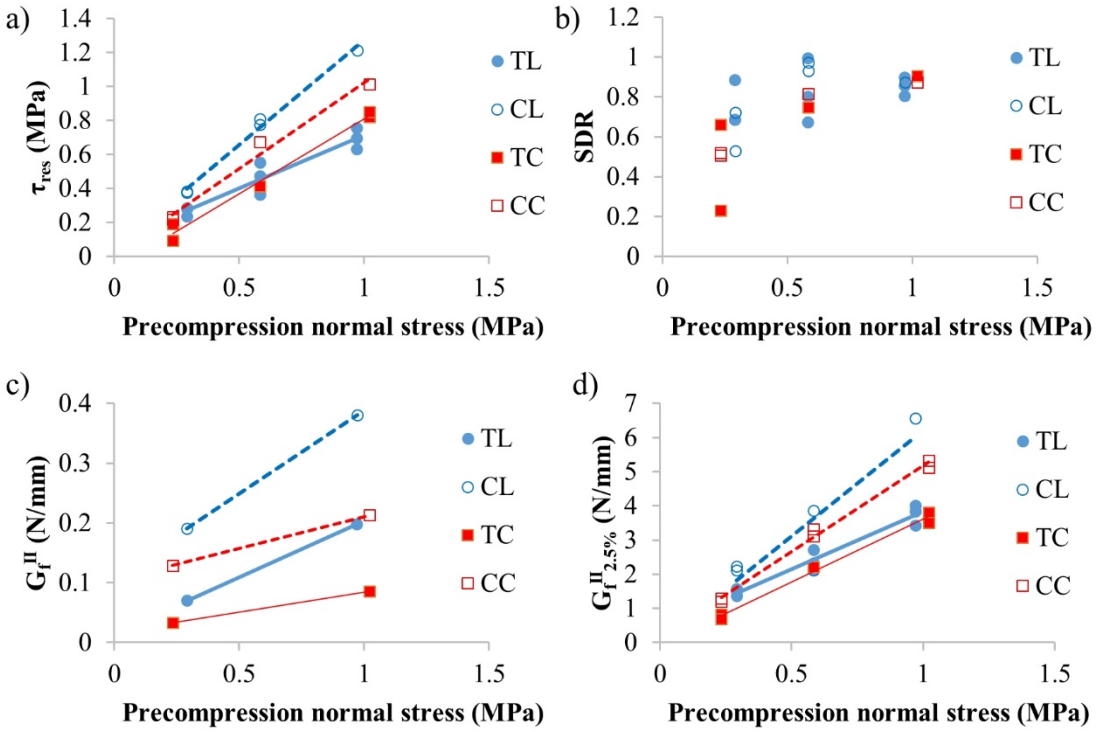

Figure 10 Comparative plots for different tested specimens of a) residual shear strength τ_{res}, b) strength degradation ratio SDR, c) cohesive fracture energy G_f^{II}, and d) cohesive-frictional fracture energy $G_{f\_2.5\%}^{II}$

3.4 Comparison with available experimental values and standards

Table 4 presents an updated literature review of experimental campaigns on masonry made with low strength mortars. A mortar compressive strength of 3.5 MPa has been selected as the top bound. Given the limited number of available references on brick masonry, stone specimens have also been considered to increase the database on historical-like materials. The table indicates, ordered by increasing mortar strength, the type of specimen tested, the mortar's binder and compressive strength, the type of unit and its compressive strength, and the shear parameters cohesion and angle of friction. The scarcity of available references is remarkable, which supports the contribution of the work presented herein. Although the majority of data were obtained from standard triplet tests, a non-negligible number of results comes from couplets or small wallettes. This fact highlights the need of

studying the correlation between different setups or, at least, defining the trends that compare results from one type of specimen to another.

The magnitude of the results of this campaign in terms of cohesion and angle of friction lay within the intervals of the other researches. As already known, there is no univocal correlation between the compressive strength of the mortar and the shear parameters as the latter depends on varied physical properties of the masonry constituents.

Table 4 Cohesion (*c*) and angle of friction (ϕ) for different types of masonry available in the literature, with compressive strengths of mortar *fm* and of units *fb*

Source	Mortar	*fm* (MPa)	Unit	*fb* (MPa)	*c* (MPa)	ϕ
Rahgozar and Hosseini [56] – Direct shear couplet	Lime	0.54	Solid clay brick	10.0	0.054	41.08º
Milosevic et al. [17] – Irregular triplet	Aerial lime	0.56	Roughly cut stones	50.0	0.080	29.24º
Rahgozar and Hosseini [56] – Direct shear couplet	Lime	0.71	Solid clay brick	10.0	0.064	41.37º
Alecci et al. [57] – Triplet	Aerial lime	0.96	Solid clay brick	17.0	0.044	-
This research – Couplet	*Hydraulic lime*	*1.02*	*Solid clay brick*	*17.99*	*0.209*	*48.08º*
This research – Triplet	*Hydraulic lime*	*1.02*	*Solid clay brick*	*17.99*	*0.167*	*33.71º*
Milosevic et al. [17] – Irregular triplet	Hydraulic lime	1.47	Roughly cut stones	50.0	0.200	50.88º
Binda et al. [58] - Triplet	Hydraulic lime	1.50	Sandstone blocks	106.0	0.330	36.46º
Binda et al. [58] - Triplet	Hydraulic lime	1.50	Calcareous stone blocks	5.9	0.580	30.12º
Pelà et al. [15] - Triplet	Aerial lime	1.63	Solid clay brick	30.7	0.040	35.65º
Uranjek and Bokan-Bosiljkov [59] – Triplet	Aerial lime + slag	2.47	Solid clay brick	32.2	0.099	43.78º
Augenti and Parisi [35] – Couplet wallette	Pozzolana	2.5	Cut tuff blocks	4.1	0.146	16.44º
This research – Couplet	*Cement*	*2.53*	*Solid clay brick*	*27.93*	*0.252*	*41.10º*
This research – Triplet	*Cement*	*2.53*	*Solid clay brick*	*27.93*	*0.165*	*36.27º*
Binda et al. [60] – Triplet	Hydraulic lime	2.61	Clay brick	14.25	0.230	30.00º
Alecci et al. [57] – Triplet	Cement-lime	2.75	Solid clay brick	17.0	0.212	-

Uranjek and Bokan-Bosiljkov [59] – Triplet	Aerial lime	2.82	Solid clay brick	32.2	0.121	38.00º
Van der Pluijm [33] – Couplet	Cement lime	3.00	Soft brick	33.00	0.100	47.55º
Van der Pluijm [33] – Couplet	Cement lime	3.00	Sandlime brick	35.00	0.150	57.87º
Alecci et al. [61] – Triplet	Cement-lime	3.22	Solid clay bricks	24.1	0.260	34.38º

Finally, Table 5 includes a comparison of the experimental results of cohesion or initial shear strength with the values recommended in two design standards: the Eurocode 6 for masonry structures [62] and the "Circolare" associated to the Italian NTC [63]. The latter is specific for existing and historical structures. Even if conceptually different, since the experimental values refer to the strength of a single joint and the design values refer to the strength of the masonry composite, the codes use the joint results to feed their models. The characteristic values of the cohesion are obtained as the 80% of the experimental results as indicated in EN1052-3 [14]. In the present research, and in the case of the weaker mortar, the characteristic initial strength is underestimated by the Eurocode 6 proposed value, while it is overestimated for the cement mortar masonry. With regard to the Italian recommendations, the experimental values lay within the suggested limits. The triplet tests, although with the associated problems of interpretation, provide values which are safer with regard to design. On the other hand, it could be expected that couplet tests might provide more representative estimations that could allow more economical and respectful interventions. Nevertheless, their representativeness should be investigated with further theoretical and numerical studies.

Table 5 Comparison of experimental results with design standard values. Average values are used for comparing with NTC [63]; characteristic values are used for comparing with EC6 [62].

Tests	Experimental cohesion *c* (MPa)	Initial shear strength NTC [63] *fv0* (MPa)	Experimental characteristic cohesion *ck* (MPa)	Characteristic initial shear strength EC6 [62] *fvk0* (MPa)
TL	0.167	0.13-0.27	0.134	0.1
CL	0.209		0.167	
TC	0.165	0.13-0.27	0.132	0.2
CC	0.252		0.202	

4 Conclusions

This paper has presented an experimental investigation on the shear characterization of masonry. A novel contribution is the execution of a direct experimental comparison between two types of specimen, standard triplets and couplets. The testing setup for couplets was a simple modification of the standard setup for triplets. Two different sets of materials were considered, with the aim of duplicating the observations.

Both types of specimen have provided sound experimental results showing the expected dependency with the normal compression stresses. This dependency influenced the values of ultimate and residual shear strengths, as well as the values of fracture energy. The magnitudes of the estimated mechanical parameters, such as cohesion, angle of friction, and cohesive fracture energy at zero precompression, are similar to those found in literature for comparable materials. In addition, both specimens have predicted similar trends with respect to dilatancy.

Couplet specimens provided consistently higher values of cohesion and angle of friction than triplets. For masonry made of handmade bricks and hydraulic lime mortar, the variations were of +25.1% and +42.6% for cohesion and angle of friction respectively. For masonry made of extruded bricks and cement mortar, the rates of increase were +69.1% and +10.2% for cohesion and angle of friction respectively. This asymmetry in the influence of the type of specimen seems to be related with

the dominant response of the materials, which is frictional in the case of the rougher handmade bricks, and cohesive in the case of the smooth extruded bricks. Therefore, a direct univocal correlation could not be found given the limited amount of data and the divergent trends. The type of specimen also influenced the estimations of fracture energy and residual shear strengths.

The differences between standard triplets and couplets could be explained as the result of several causes. First, the stress distributions along the mortar joints are different in both types of specimen. Second, the lower strengths found with triplets could be explained from a statistical approach, given that the brick-mortar interface area is twice larger in triplets than in couplets. Third, the evaluation of the actual stresses along the joints may be biased in both types of specimen, by the double peak phenomenon in the case of triplets, and by the friction of the lateral faces in the case of couplets.

According to the obtained results and the existing literature, it is recommended to use triplets as general-purpose shear characterisation testing setup because their use is more widespread and they are prescribed by the standards. Couplets have proven to be able to become a possible alternative configuration. However, this work is a preliminary study of a setup under development and a number of improvements have still to be introduced in order to get reliable results. At the moment, couplets would only be advisable for those cases whose material consumption has to be reduced to the maximum, for example, if applied to historical buildings and recovered constituents. Further research involving both experimental and numerical methods is needed, in any case, to improve the possible correlation between types of specimen and, in general, to find enhanced ways to determine the shear parameters of masonry.

A database of shear parameters for masonry made with low strength mortars has been presented. Besides results on standard triplets, the database included results from couplets and other irregular specimens, which are easily found in literature. It was however difficult to find references

with experimental comparisons between the different types of specimen. This is a consideration that should be kept in mind when using parameters from existing databases. It is always necessary to know the conditions under which those parameters were obtained.

One of the studied sets of materials aimed to represent a historical type of masonry built of handmade bricks and hydraulic lime mortar. The standard triplet tests provided a cohesion of 0.167 MPa and an angle of friction of 33.71º. These new results contribute to complete the available database on similar materials.

Acknowledgements

The authors gratefully acknowledge the financial support from the Ministry of Science, Innovation and Universities of the Spanish Government (MCIU), the State Agency of Research (AEI), as well as that of the ERDF (European Regional Development Fund) through the project SEVERUS (Multilevel evaluation of seismic vulnerability and risk mitigation of masonry buildings in resilient historical urban centres, ref. num. RTI2018-099589-B-I00). Support from Secretaria d'Universitats i Investigació de la Generalitat de Catalunya through a predoctoral grant awarded to the first author is gratefully acknowledged. Support from Universitat Politècnica de Catalunya through a predoctoral grant awarded to the third author is also acknowledged.

The authors wish to thank Paolo Casadei, José Luis Sánchez and Patricio Contreras from KERAKOLL for providing part of the materials used in the experimental campaign.

References

[1] R.H. Atkinson, B.P. Amadei, S. Saeb, S. Sture, Response of masonry bed joints in direct shear, J. Struct. Eng. 115 (1989) 2276–2296. doi:10.5940/jcrsj.32.Supplement_78.

[2] M. Tomaževič, Shear resistance of masonry walls and Eurocode 6: Shear versus tensile strength of masonry, Mater. Struct. Constr. 42 (2009) 889–907. doi:10.1617/s11527-008-9430-6.

[3] J.R. Riddington, P. Jukes, A comparison between panel, joint and code shear strength, in: N.G. Shrive, A. Huizer (Eds.), 10th Int. Brick Block Mason. Conf., Masonry Council of Canada, 1994: pp. 1481–1490. doi:10.1017/CBO9781107415324.004.

[4] S. Zhang, K. Beyer, Numerical investigation of the role of masonry typology on shear strength, Eng. Struct. 192 (2019) 86–102. doi:10.1016/j.engstruct.2019.04.026.

[5] D. Malomo, M.J. DeJong, A. Penna, Influence of bond pattern on the in-plane behaviour of URM piers, Int. J. Archit. Herit. 00 (2019) 1–20. doi:10.1080/15583058.2019.1702738.

[6] P. Jukes, An investigation into the shear strength of masonry joints, PhD Thesis, University of Sussex, 1997.

[7] P. Jukes, J. Riddington, A review of masonry joint shear strength test methods, Mason. Int. 11 (1997) 37–43.

[8] M. Montazerolghaem, W. Jaeger, A Comparative Numerical Evaluation of Masonry Initial Shear Test Methods and Modifications Proposed for EN 1052-3, in: 9th Int. Mason. Conf., 2014: pp. 1–10.

[9] R. Popal, A New Shear Test Method for Mortar Bed Joints, Dissertation, University of Calgary, 2013.

[10] J.R. Riddington, K.H. Fong, P. Jukes, Numerical study of failure initiation in different joint shear stests, Mason. Int. 11 (1997) 44–50.

[11] R. Popal, S.L. Lissel, Numerical evaluation of existing mortar joint shear tests and a new test method, in: 8th Int. Mason. Conf., 2010: pp. 795–802.

[12] P.B. Lourenço, L.F. Ramos, Characterization of cyclic behavior of dry masonry joints, J. Struct. Eng. 130 (2004) 779–786. doi:10.1061/(ASCE)0733-9445(2004)130.

[13] A.T. Vermeltfoort, Shear Strength Variation Due To Mortar Strength Variation and the Use of a Triplet Shear Test Set-Up, in: 15th Int. Brick Block Mason. Conf., 2012.

[14] European Committee for Standardization (CEN), EN 1052-3 Methods of test for masonry - Part 3: Determination of initial shear strength, (2007).

[15] L. Pelà, K. Kasioumi, P. Roca, Experimental evaluation of the shear strength of aerial lime mortar brickwork by standard tests on triplets and non-standard tests on core samples, Eng. Struct. 136 (2017) 441–453. doi:10.1016/j.engstruct.2017.01.028.

[16] O.P. Cavalheiro, G.M. Pedroso, Experimental data on hollow block prisms using direct shear test, in: 12th Int.

Brick/Block Mason. Conf., 2000: pp. 433–440.

[17] J. Milosevic, A.S. Gago, M. Lopes, R. Bento, Experimental assessment of shear strength parameters on rubble stone masonry specimens, Constr. Build. Mater. 47 (2013) 1372–1380. doi:10.1016/j.conbuildmat.2013.06.036.

[18] D.-H. Jiang, X.-S. Xiao, A New Masonry Shear Test Method Determining, in: 10th Int. Brick Block Mason. Conf., 1994: pp. 1013–1020.

[19] G. Andreotti, F. Graziotti, G. Magenes, Expansion of mortar joints in direct shear tests of masonry samples: implications on shear strength and experimental characterization of dilatancy, Mater. Struct. Constr. 52 (2019) 1–16. doi:10.1617/s11527-019-1366-5.

[20] S. Zhang, N. Richart, K. Beyer, Numerical evaluation of test setups for determining the shear strength of masonry, Mater. Struct. Constr. 51 (2018) 1–12. doi:10.1617/s11527-018-1236-6.

[21] F. Ferretti, C. Mazzotti, R. Esposito, J.G. Rots, Shear-sliding behavior of masonry: Numerical micro-modeling of triplet tests, in: G. Meschke, B. Pichler, J.G. Rots (Eds.), Comput. Model. Concr. Struct. - Proc. Conf. Comput. Model. Concr. Concr. Struct. EURO-C 2018, CRCPress, 2018: pp. 941–954. doi:10.1201/9781315182964-109.

[22] D. Marastoni, Advanced Minor Destructive Testing for the Assessment of Existing Masonry, PhD Thesis, Università di Bologna, 2016.

[23] P.B. Lourenco, J.O. Barros, J.T. Oliveira, Shear testing of stack bonded masonry, Constr. Build. Mater. 18 (2004) 125–132. doi:10.1016/j.conbuildmat.2003.08.018.

[24] G. Vasconcelos, P.B. Lourenço, Experimental characterization of stone masonry in shear and compression, Constr. Build. Mater. 23 (2009) 3337–3345. doi:10.1016/j.conbuildmat.2009.06.045.

[25] M. Angelillo, P.B. Lourenço, G. Milani, Masonry behaviour and modelling, in: Mech. Mason. Struct., Springer, 2014. doi:10.1007/978-3-7091-1774-3.

[26] J.R. Riddington, P. Jukes, A masonry joint shear strength test method, Proc. Inst. Civ. Eng. Struct. Build. 104 (1994) 267–274. doi:10.1680/istbu.1994.26777.

[27] C.K. Murthy, A.W. Hendry, Preliminary investigation of the shear strength of one-sixth scale model brickwork, 1965.

[28] B.P. Sinha, A.W. Hendry, Further investigations of bond tension, bond shear and the effect of precompression on shear strength of model brick masonry couplets, Br. Ceram. Res. Assoc. March (1966).

[29] J.C.G. Chin Wah, Shear resistance of masonry walls, PhD Thesis, University of London, 1972.

[30] S.J. Lawrence, Couplet and triplet tests for the measurement of bond strength of brickwork, Experimental Building Station, 1977.

[31] S. Stöckl, P. Hofmann, Tests on the shear bond behaviour in the bed-joints of masonry, in: J. De Courzy (Ed.), 8th Int. Brick Block Mason. Conf., Elsevier, 1986: pp. 292–303.

[32] P. Roca, G. Araiza, Shear response of brick masonry small assemblages strengthened with bonded FRP laminates for in-plane reinforcement, Constr. Build. Mater. 24 (2010) 1372–1384. doi:10.1016/j.conbuildmat.2010.01.005.

[33] R. Van Der Pluijm, Shear behaviour of bed joints, in: 6th North Am. Mason. Conf., 1993: pp. 125–136.

[34] A. Rahman, T. Ueda, Experimental investigation and numerical modeling of peak shear stress of Brick Masonry mortar joint under compression, J. Mater. Civ. Eng. 26 (2014) 1–13. doi:10.1061/(ASCE)MT.1943-5533.0000958.

[35] N. Augenti, F. Parisi, Constitutive modelling of tuff masonry in direct shear, Constr. Build. Mater. 25 (2011) 1612–1620. doi:10.1016/j.conbuildmat.2010.10.002.

[36] P. Schubert, A. Caballero Gonzalez, Vergleichende Untersuchungen nach DIN 18555-5 und DIN EN 1052-3. Part 1 and Part 2. Research reports F449 and F449/2, 1996.

[37] F. Fouchal, F. Lebon, I. Titeux, Contribution to the modelling of interfaces in masonry construction, Constr. Build. Mater. 23 (2009) 2428–2441. doi:10.1016/j.conbuildmat.2008.10.011.

[38] J. Segura, D. Aponte, L. Pelà, P. Roca, Influence of recycled limestone filler additions on the mechanical behaviour of commercial premixed hydraulic lime based mortars, Constr. Build. Mater. 238 (2020) 117722. doi:10.1016/j.conbuildmat.2019.117722.

[39] J. Segura, L. Pelà, P. Roca, Monotonic and cyclic testing of clay brick and lime mortar masonry in compression, Constr. Build. Mater. 193 (2018) 453–466. doi:10.1016/j.conbuildmat.2018.10.198.

[40] E. Bernat-Maso, Analysis of unreinforced and TRM-strengthened brick masonry walls subjected to eccentric axial load, PhD Thesis, Universitat Politècnica de Catalunya, 2014.

[41] European Committee for Standardization (CEN), EN 772-1:2011 Methods of Test for Masonry Units - Part 1: Determination of Compressive Strength, (2011).

[42] European Committee for Standardization (CEN), EN 772-6 Methods of test for masonry units - Part 6: Determination of bending tensile strength of aggregate concrete masonry units, (2002).

[43] European Committee for Standardization (CEN), EN 772-21 Methods of test for masonry units - Part 21: Determination of water absorption of clay and calcium silicate masonry units by cold water absorption, (2011).

[44] European Committee for Standardization (CEN), EN 1015-11 Methods of test for mortar for masonry - Part 11: Determination of flexural and compressive strength of hardened mortar, (1999).

[45] J. Segura, L. Pelà, P. Roca, A. Cabané, Experimental analysis of the size effect on the compressive behaviour of cylindrical samples core-drilled from existing brick masonry, Constr. Build. Mater. 228 (2019) 116759. doi:10.1016/j.conbuildmat.2019.116759.

[46] ACI, ASCE, TMS, ACI 530.1-11/ASCE 5-11/TMS 402-11 Building Code Requirements for Masonry Structures, (2005).

[47] P.B. Lourenço, J.G. Rots, Multisurface interface model for analysis of masonry structures, J. Eng. Mech. (1997) 660–668. doi:10.1061/(ASCE)0733-9399(1997)123.

[48] A.M. D'Altri, V. Sarhosis, G. Milani, J. Rots, S. Cattari, S. Lagomarsino, E. Sacco, A. Tralli, G. Castellazzi, S. de Miranda, Modeling Strategies for the Computational Analysis of Unreinforced Masonry Structures: Review and Classification, Arch. Comput. Methods Eng. (2019). doi:10.1007/s11831-019-09351-x.

[49] P.B. Lourenço, Computational strategies for masonry structures, PhD Thesis, Delft University of Technology, 1996.

[50] M. Bisoffi-Sauve, S. Morel, F. Dubois, Modelling mixed mode fracture of mortar joints in masonry buildings, Eng. Struct. 182 (2019) 316–330. doi:10.1016/j.engstruct.2018.11.064.

[51] G.P.A.G. van Zijl, Modeling masonry shear-compression: Role of dilatancy highlighted, J. Eng. Mech. 130 (2004) 1289–1296. doi:10.1061/(ASCE)0733-9399(2004)130:11(1289).

[52] N. Mojsilović, M. Petrović, X.R. Anglada, Masonry elements with multi-layer bed joints: Behaviour under monotonic and static-cyclic shear, Constr. Build. Mater. 100 (2015) 149–162. doi:10.1016/j.conbuildmat.2015.09.065.

[53] S. Ali, A.W. Page, A failure criterion for mortar joints in brickwork subjected to combined shear and tension, Mason. Int. 9 (1986) 43–54.

[54] W.S. Lei, A generalized weakest-link model for size effect on strength of quasi-brittle materials, J. Mater. Sci. 53 (2018) 1227–1245. doi:10.1007/s10853-017-1574-8.

[55] M. Shadlou, E. Ahmadi, M.M. Kashani, Micromechanical modelling of mortar joints and brick-mortar interfaces in masonry Structures: A review of recent developments, Structures. 23 (2020) 831–844. doi:10.1016/j.istruc.2019.12.017.

[56] A. Rahgozar, A. Hosseini, Experimental and numerical assessment of in-plane monotonic response of ancient mortar brick masonry, Constr. Build. Mater. 155 (2017) 892–909. doi:10.1016/j.conbuildmat.2017.08.079.

[57] V. Alecci, M. Fagone, T. Rotunno, M. De Stefano, Shear strength of brick masonry walls assembled with different types of mortar, Constr. Build. Mater. 40 (2013) 1038–1045. doi:10.1016/j.conbuildmat.2012.11.107.

[58] L. Binda, A. Fontana, G. Mirabella, Mechanical behavior and stress distribution in multiple-leaf stone walls, in: 10th Int. Brick Block Mason. Conf., 1994: pp. 51–59.

[59] M. Uranjek, V. Bokan-Bosiljkov, Influence of freeze-thaw cycles on mechanical properties of historical brick masonry, Constr. Build. Mater. 84 (2015) 416–428. doi:10.1016/j.conbuildmat.2015.03.077.

[60] L. Binda, G. Mirabella Roberti, C. Tiraboschi, S. Abbaneo, Measuring Masonry Material Properties, U.S.-Italy Work. Guidel. Seism. Eval. Rehabil. Unreinforced Mason. Build. (1994) 326–347. doi:10.1017/CBO9781107415324.004.

[61] V. Alecci, F. Focacci, L. Rovero, G. Stipo, M. De Stefano, Intrados strengthening of brick masonry arches with different FRCM composites: Experimental and analytical investigations, Compos. Struct. 176 (2017) 898–909. doi:10.1016/j.compstruct.2017.06.023.

[62] European Committee for Standardization (CEN), Eurocode 6: Design of masonry structures - Part 1: General rules for reinforced and unreinforced masonry structures, (2005).

[63] Ministero delle Infrastrutture e dei Trasporti, Circolare 21 gennaio 2019 Istruzioni per l'applicazione dell' "Aggiornamento delle 'Norme techniche per le costruzioni'" di cui al decreto ministeriale 17 gennaio 2018, (2019). https://www.gazzettaufficiale.it/eli/gu/2019/02/11/35/so/5/sg/pdf.